

Contact probe radius compensation using computer aided design models

M Ristic*, I Ainsworth and D Brujic

Mechanical Engineering Department, Imperial College of Science, Technology and Medicine, London, UK

Abstract: Probe radius compensation is necessary in metrology applications that employ contact probes, but it can be a significant source of systematic measurement errors when dealing with free-form part geometry. The paper presents implementation and performance analysis of a proposed new compensation technique based on the nominal computer aided design (CAD) model, which is assumed to be defined using non-uniform rational B -splines (NURBS). Errors associated with the conventional compensation approach are assessed on the basis of experiments using a modern coordinate measuring machine (CMM), providing clear motivation for this work. The proposed method consists of a number of steps, including measurement, generation of offset nominal surfaces, registration, surface fitting, data smoothing and calculation of compensating offsets. Critical steps include registration and NURBS surface fitting and their implementation is presented. Simulation studies are used to analyse the registration accuracy and the accuracy of the overall method in comparison with the conventional one. The proposed method is shown to produce superior results in situations involving non-uniform measurement distribution, measurement noise, free-form geometry with no clear datums, deformation relative to the nominal shape and component misalignment.

Keywords: probe compensation, coordinate measuring machine (CMM), non-uniform rational B -splines (NURBS)

NOTATION

f surface fitting cost function
 F registration cost function
 N basis functions
 N surface normal
 O surface offset
 p the degree of a surface in the first parametric direction
 P control points
 q the degree of a surface in the second parametric direction
 R rational basis functions
 T surface tangent
 u parametric knot value in the first surface direction
 U parametric knot vector in the first surface direction
 v parametric knot value in the second surface direction

V parametric knot vector in the second surface direction
 w control point weights

1 INTRODUCTION

A significant proportion of parts in aerospace and automotive industries comprise free-form shapes, which are commonly modelled using non-uniform rational B -splines (NURBS). Examples include aeroengine components, car body panels and various dies [1, 2]. Dimensional measurement of such parts is generally performed as part of:

- (a) product and manufacturing process development and
- (b) quality control.

Today, the standard instrument for dimensional metrology is the coordinate measuring machine (CMM) equipped with a touch trigger probe. However, measurement of free-form parts is non-trivial in view of the shape complexity, the frequent lack of adequate reference features (datums) and the large number of

The MS was received on 23 December 1999 and was accepted after revision for publication on 29 August 2000.

*Corresponding author: Mechanical Engineering Department, Imperial College of Science, Technology and Medicine, Exhibition Road, London SW7 2BX, UK.

measurements that is often required to characterize the part shape adequately.

In recent years these difficulties have led some metrology practitioners in the industry to consider the adoption of non-contact scanning devices for metrology purposes, such as those based on laser lighting or structured light. However, those devices generally offer inferior accuracy compared with the conventional CMM equipped with a contact probe. For each measured point, accuracy in the region 50–100 μm is achievable using laser triangulation sensors, while that in the region 2–3 μm is achievable using the CMM with touch trigger probe. Thus for the majority of those in the industry involved in precision dimensional metrology the CMM and the contact probe still represent the instruments of choice [3].

The CMM is also becoming increasingly attractive for measurement of free-form shapes owing to some recent developments [4] which make them better suited for collection of dense measurement sets. These developments include the use of analogue probes, which offer greatly increased measuring range and facilitate the development of automated scanning procedures based on surface following. Furthermore, new CMM control techniques are available, which enable CMMs equipped with a touch trigger probe to scan the surface in a similar fashion in acceptable time. In addition, computer aided design (CAD) based techniques for measurement planning enable accurate control of the CMM and optimization of the measurement process in relation to various parameters, even for very complicated shapes [5].

However, the need for probe radius compensation remains an important obstacle for using contact systems to measure free-form geometry [6, 7]. This arises from the fact that the probe tip is a sphere of a finite radius (Fig. 1). Consequently the CMM can record only the coordinates of the sphere centre and not those of the point of contact.

The conventional compensation method is to assume that the direction of the surface normal at the point of contact is *a priori* known. Usually the CMM is programmed to approach the surface in that direction and the compensation offset is applied accordingly. There are subtle variations in which different CMM manufacturers implement this functionality but those details are largely undisclosed. However, this conventional compensation method may be a significant source of errors, as will be demonstrated in the next section. Essentially, any deformation of the component relative to its nominal shape and any misalignment relative to its assumed location in the measuring machine will result in erroneous estimate of the surface normal direction at the point of contact and therefore in erroneous compensation offset.

This problem has been addressed by some researchers. Most notably, Mayer *et al.* [7] propose interpolation of the raw (uncompensated) data using Kriging. The interpolated surface is taken to represent the offset of the actual part surface, where the offset is equal to the radius of the sphere at the probe tip. Normal directions are calculated on the interpolated surface and compensation is then applied in that direction.

The main limitation of the interpolation method, however, is that the data must be ordered and that the magnitude of the measurement noise is negligible, especially in relation to point density. The ordering of the data generated by most systems based on surface following is often ambiguous and misleading, owing to the way in which surface following algorithms operate. Furthermore, in practice one often has to deal with data which were not collected in a prescribed sequence but are in all other respects a valid measurement set.

This paper proposes a compensation approach which was designed to operate accurately and reliably under the following conditions:

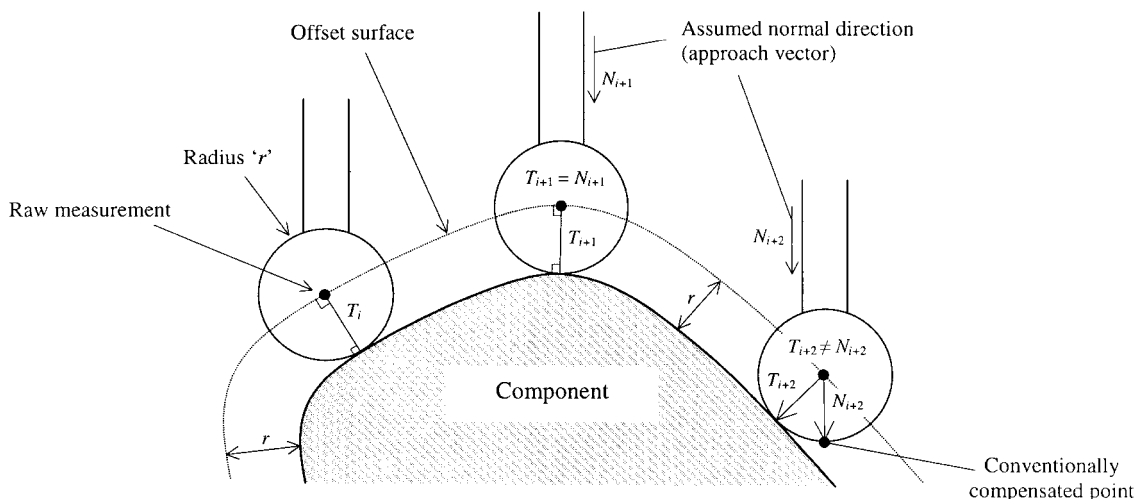


Fig. 1 Conventional and offset surface compensation

- (a) free-form geometry of the part;
- (b) absence of clear reference features;
- (c) non-uniform (random) distribution of measured points;
- (d) deformation of the actual shape relative to the nominal (assumed) shape;
- (e) misalignment of the object in relation to its assumed position in the CMM;
- (f) presence of measurement noise.

The compensation approach is based on fitting a surface through the raw measurement data. Because surface fitting to unorganized data is a difficult problem, the available CAD model of the part is utilized, which is assumed to consist of NURBS entities. The proposed method consists of several distinct steps, namely measurement, generation of offset nominal surfaces, registration, surface fitting, data smoothing and calculation of compensating offsets.

The paper is structured in the following fashion. The next section provides an analysis of the conventional approach for probe radius compensation in relation to the measurement of free-form shapes, showing that the associated systematic errors are significant in relation to the achievable accuracy of the CMM, thus providing a clear motivation for this work. The outline of the proposed compensation method is provided in Section 3. Since NURBS modelling forms the basis of the CAD-based method, Section 4 provides an overview of the NURBS formulation and the most relevant operations on them. Since accurate registration is one of the cornerstones of the proposed method, Section 5 presents its implementation and analyses the achieved accuracy on the basis of Monte Carlo simulation. The details of the implemented method for NURBS surface fitting to an unorganized point set are provided in Section 6. Finally, Section 7 presents the simulation studies that were conducted in order to validate the proposed method and to assess its accuracy. The performance is analysed in comparison with the conventional methodology and in relation to factors such as the measurement noise, misalignment and the deformation of the actual shape relative to its nominal CAD model.

2 THE CONVENTIONAL COMPENSATION METHOD

A typical automated measurement command using a mainstream CMM instruction language such as Dimensional Measurement Interface Standard [8] would take the following form:

```
PTMEAS, x, y, z, i, j, k
```

This command instructs the CMM to measure a point located at the position (x, y, z) and specifies the direction of approach vector (i, j, k) . The approach vector is

typically specified on the basis of the nominal model of the component being measured and the referencing which establishes the location of the actual part in the CMM. Once the point measurement has been taken and the centre of the sphere at the probe tip (raw measurement) has been recorded, the compensation is calculated by translating the recorded raw measurement by the distance equal to the probe tip radius in the direction (i, j, k) [1]. Thus the conventional compensation makes a fundamental assumption that the nominal normal vector is the same as the actual one, at the actual point contact between the probe and the part.

Although this method represents a simple, robust and relatively effective form of compensation, it can be a significant source of systematic measurement error. The problem lies in the fact that the assumed normal is obtained from the nominal model and relates to the nominal model's global coordinate frame. Hence, if there is misalignment between the coordinate frame of the nominal and that of the component located in the CMM, or if the shape of the actual component differs from that of the nominal, then there is a high probability that the assumed normals will be incorrect. Figure 1 illustrates the error between assumed normal N_{i+2} and the true normal T_{i+2} that can result from conventional compensation.

The magnitude of the systematic error introduced by compensation clearly depends on a number of factors, including the probe tip radius, local radius of curvature of the component, component misalignment due to referencing errors and, importantly, deformation of the actual component shape relative to its nominal (assumed) shape. However, compensation error is not the only error introduced during measurement. Systematic and random noise introduced by the CMM hardware are also present.

In order to gain a fuller insight into this situation, tests were conducted using a modern computer numerical control (CNC) CMM and the performance was analysed. The machine used was LK G-90C equipped with a Renishaw PH-10M motorized indexing head and a Renishaw TP2-5W touch trigger probe. The CMM is controlled by a dedicated control computer running the full suite of measurement software. The investigation took the form of measuring a section of a cylinder perpendicular to its axis of symmetry, as illustrated in Fig. 2. A cylinder was used because it represented a shape that can be readily manufactured to a very high tolerance; it allowed analytical estimation of the compensation error, while also allowing investigation of the influences of the identified factors.

A characteristic measurement set is shown in Fig. 3. The probe tip radius was 1 mm, and the radius of the cylinder was 10 mm. In order to demonstrate compensation error a gross misalignment of 2 mm (d_y) was introduced as shown in Fig. 2, and 500 measurements were taken at uniform intervals when the probe approach angle α was between 0° and 180° .

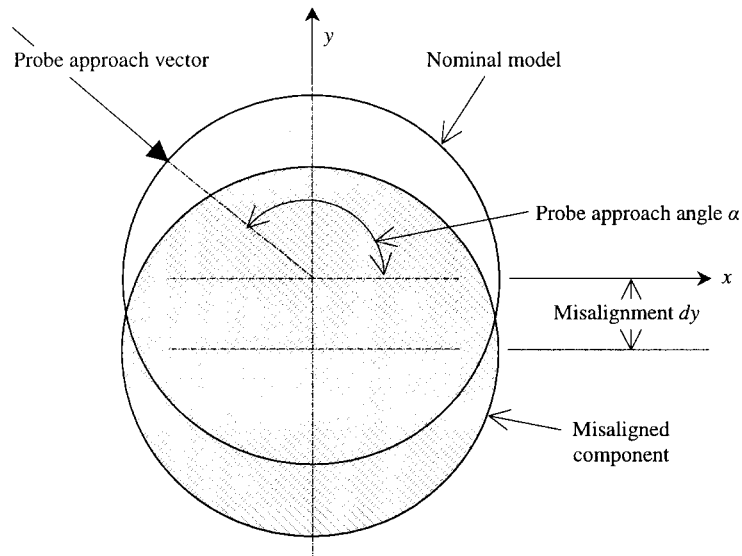


Fig. 2 Schematic of measuring section of a cylinder with misalignment

2.1 Analytical calculation of compensation error

Figure 4 expands the schematic of Fig. 2 and shows the geometry required to analyse the conventional compensation procedure. The corresponding compensation error may be evaluated analytically by first finding the intersection between the offset model and the nominal normal using the following equations:

$$y = x \tan \alpha \quad (1)$$

$$x^2 + (y + dy)^2 = (R + r)^2 \quad (2)$$

where α is the angle of the nominal normal (probe tip approach vector). The solution of equations (1) and (2) will yield x_{raw} and y_{raw} , the raw measurement point. Next, translate the raw point in the direction of the nominal normal for a distance equal to r the probe tip radius. This will yield x_{comp} and y_{comp} , which represent the measurement point location that would have been obtained using conventional compensation. The error in compensation is represented by the distance between $(x, y)_{\text{comp}}$ and the closest point on the actual component $(x, y)_{\text{closest}}$. To find the point $(x, y)_{\text{closest}}$ the following

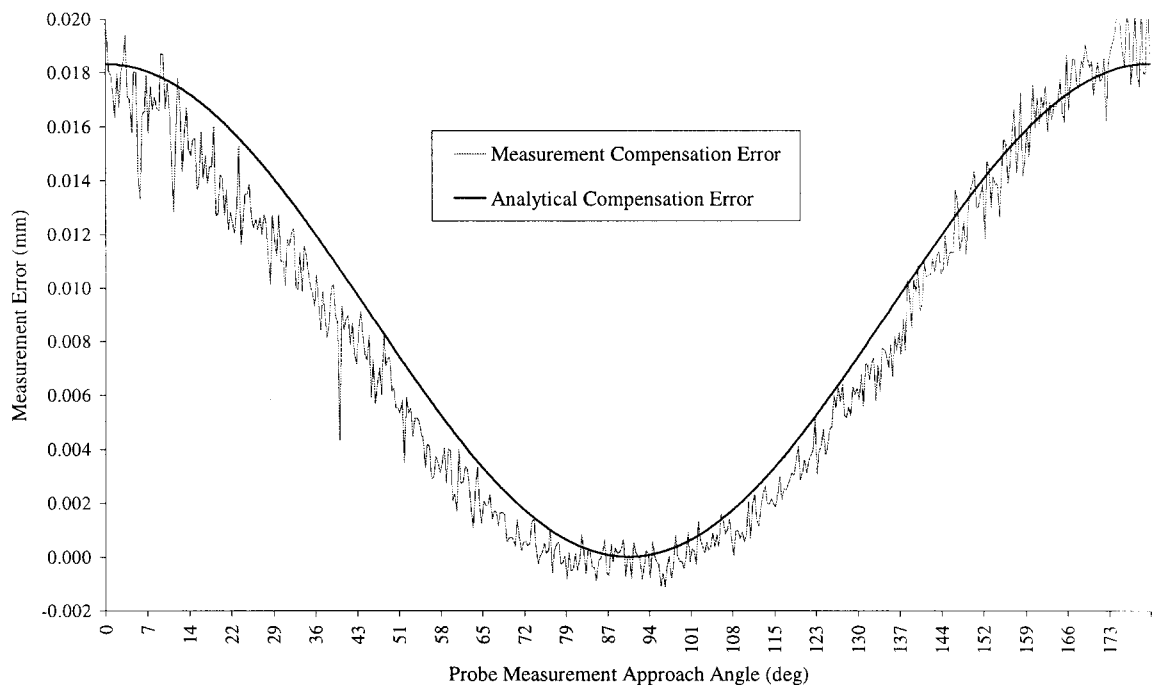


Fig. 3 Measurement error versus probe approach angle, produced by conventional compensation

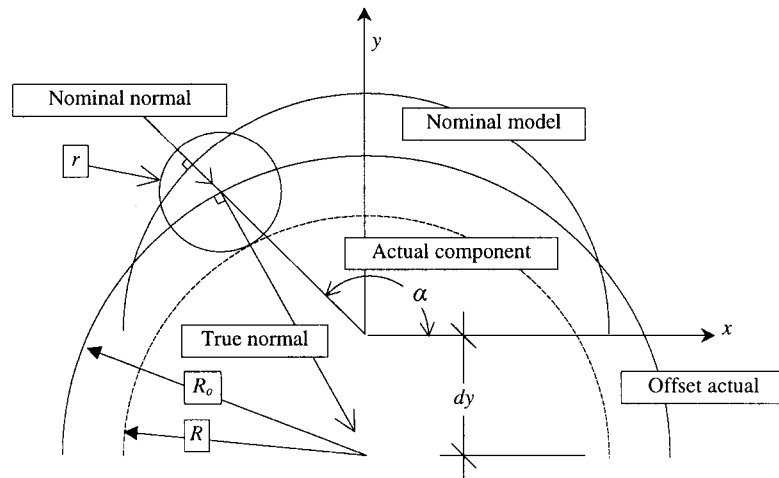


Fig. 4 Geometry of measurement with misalignment

equations were solved:

$$y = \frac{y_{\text{comp}} + dy}{x_{\text{comp}}} x - dy \quad (3)$$

$$x^2 + (y + dy)^2 = R^2 \quad (4)$$

Equation (3) represents the line that would pass through the compensated point $(x, y)_{\text{comp}}$ and the centre of the actual component, and equation (4) represents the surface of the actual component. Finally the distance between $(x, y)_{\text{comp}}$ and $(x, y)_{\text{closest}}$ would give the magnitude of compensation error that could be expected when using the conventional method.

2.2 Experimental evaluation of the measurement error

Figure 3 presents two curves: the first, 'Measurement Compensation Error', shows the actual results that were obtained using the CMM under the prescribed conditions; the second shows the analytically calculated estimate of the expected compensation error. The figure shows that the error component introduced by conventional compensation is by far the most significant. It also shows that there exists a random component of measurement noise that is not negligible. The final observation from Fig. 4 is that there is a second component of systematic error introduced, which is most prominent when α is between 15° and 55° . Although full analysis of this error component has yet to be performed, initial investigations suggest that it is due to the mechanical configuration of the contact probe's touch sensitive switch.

The graph of Fig. 5 was constructed in order to calculate the maximum compensation error that could be expected for different sizes of probe tip and various component radii of curvature. Letting r be the probe tip radius and R the measured component's local radius of curvature; then, using the value of r/R , the

maximum compensation error can be obtained from this graph, for various magnitudes of misalignment. As an example, if the radius of curvature of the component R is 10 mm and the radius of the probe tip r is 3 mm, then r/R will be equal to 0.3; assuming a displacement of 1.62 mm shows that the maximum compensation error would be in the region of 0.03 mm (or $30 \mu\text{m}$). The compensation error introduced by misalignment and component deformation can be accounted for by the differences between the assumed surface normal and the true surface normal at the measurement location. Generally both factors will influence all measurement undertaken using a CMM.

3 THE PROPOSED COMPENSATION METHOD

The steps in the proposed methodology are presented with reference to Fig. 6. It differs fundamentally from the conventional approach in that the compensation is calculated and applied after the full measurement data set has been obtained, rather than on a point-by-point basis.

Step 1: measurement. As Fig. 6 indicates, the planning and the execution of the measurement process will be typically, although not necessarily, performed on the basis of the nominal CAD model of the part in question. The establishment of the component location in the CMM is performed as part of this task. In situations when suitable reference features are available, those features may be employed for component location in a conventional way, for example through measurement of three, two and one point on a feature comprising three mutually orthogonal flat faces [1]. In situations when such reference features are not available, the component location may be established through the registration procedure described below. In either case, the result of the measurement process

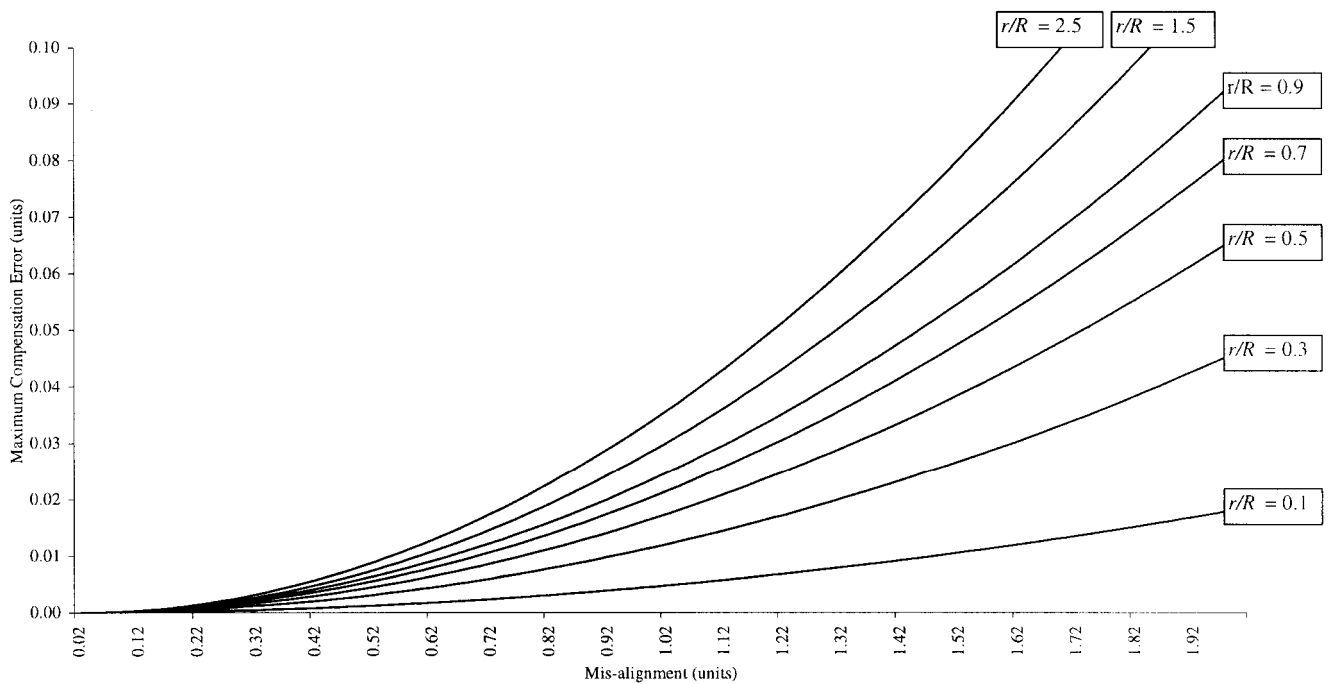


Fig. 5 Compensation error versus misalignment for different r/R values, produced by conventional compensation. r , probe radius; R , local radius of curvature of the surface

is a set of raw measurement data, represented by the coordinates of the recorded positions of the probe tip centre.

Step 2: registration. Using the measured data points and the nominal CAD model as the input, registration is the process which establishes point correspondences between these two entities and calculates the transfor-

mation (rotation/translation) which aligns them. Since the measured data at this stage consist of points that are offset from the actual points of contact by the length of the probe tip radius, offset entities of the nominal CAD model for registration are employed. This approach is in contrast to the conventional one in two respects. First, it is the raw, uncompensated

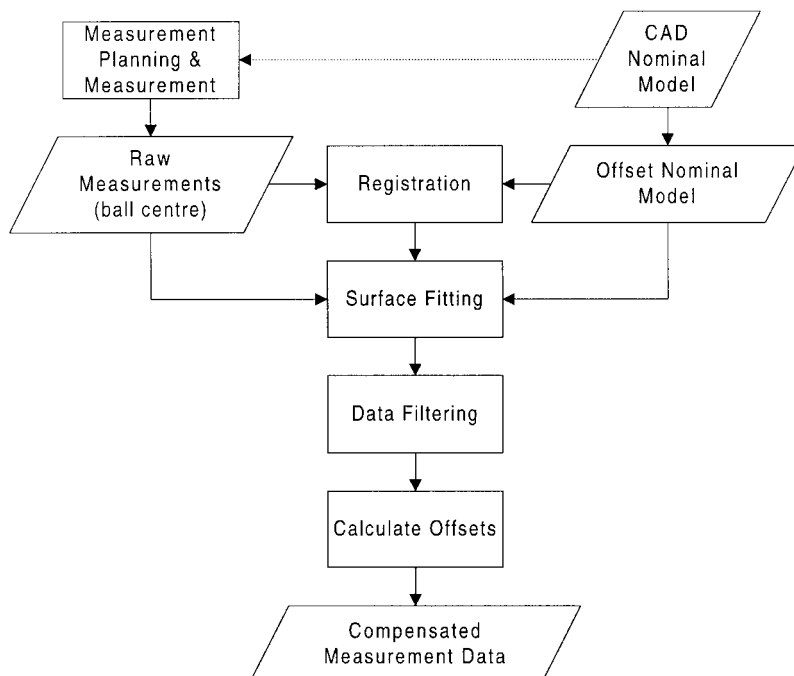


Fig. 6 Proposed compensation method

data that are employed for registration, so registration accuracy is unaffected by any compensation errors. Second, it is proposed that all the measured data be used for registration. Considering that a large number of points is usually collected during dimensional measurement of free-form shapes, the registration accuracy and the confidence in registration results will be greatly improved by this, especially in the presence of measurement noise.

Step 3: surface fitting. The next step in the procedure is surface fitting through the raw data. In general three-dimensional surface fitting requires careful consideration in choosing the appropriate surface type, such that it meets the accuracy requirements while also being able to perform well in the presence of noise contained in the data. Robustness and computational efficiency of the fitting process are important practical considerations. In this work, NURBS surfaces clearly offer an attractive choice for the fitted surface for a number of reasons. First, as the nominal CAD model of the part is defined using NURBS, it provides a good initial approximation for the fitting. Thus the often difficult choice of parameters such as surface order, number of control points and weights can be made on the basis of the existing nominal model. Second, data parametrization can also be readily performed on the basis of the nominal model, as part of the preceding registration step. Finally, significant differences between the actual and nominal object shapes can be readily accommodated using knot insertion to increase local surface flexibility. Following this, surface fitting is performed by using the previously calculated offset nominal surfaces as the initial guess, while the measured raw points are parametrized according to their corresponding nominal points. Fitting involves calculation of the control point positions that achieve least-squares fit between the surface and the data. The implementation of this procedure is explained in more detail in Section 6.

Step 4: data smoothing. Experimental data presented in Fig. 3 clearly show that measurement noise may be significant. For this reason data smoothing is proposed as the next step, which is achieved by replacing all of the raw measurement points with their closest points on the fitted surface.

Step 5: calculation of offsets. The final step in the procedure is the actual calculation of the offsets for each point. For each measured point, the normal vector on the fitted surface is calculated and the offset equal to probe radius is applied in that direction to calculate the coordinates of the actual point of contact.

It is evident that the registration and surface fitting steps are the most important and difficult ones. These are explained below, following a brief overview of NURBS definition and main NURBS functions.

4 NURBS AS THE PRIMARY MODELLING ENTITY

The main reason for adopting NURBS as the CAD modelling entity is the fact that they have been widely accepted as an industry standard [2, 9]. Furthermore, NURBS provide the basis for geometric data exchange with existing CAD systems, because they can precisely represent all relevant shapes including natural quadric shapes such as cylinders and cones. NURBS are also supported by the Initial Graphics Exchange Specification [10] file format.

4.1 NURBS definition

A NURBS surface of degree p in the u direction and degree q in the v direction is a bivariate vector-valued piecewise rational function of the form

$$\begin{aligned} \mathbf{S}(u, v) &= [x_s(u, v), y_s(u, v), z_s(u, v)] \\ &= \frac{\sum_{i=0}^n \sum_{j=0}^m N_{i,p}(u) N_{j,q}(v) w_{i,j} \mathbf{P}_{i,j}}{\sum_{i=0}^n \sum_{j=0}^m N_{i,p}(u) N_{j,q}(v) w_{i,j}}, \quad 0 \leq u, v \leq 1 \end{aligned} \quad (5)$$

where the control points $\{\mathbf{P}_{i,j}\}$ form a bi-directional control net and $\{w_{i,j}\}$ are control point weights. The functions $\{N_{i,p}(u)\}$ and $\{N_{j,q}(v)\}$ are the non-rational B -spline basis functions defined on the knot vectors

$$\begin{aligned} \mathbf{U} &= (\underbrace{0, \dots, 0}_{p+1}, u_{p+1}, \dots, u_{r-p-1}, \underbrace{1, \dots, 1}_{p+1}) \\ \mathbf{V} &= (\underbrace{0, \dots, 0}_{q+1}, v_{q+1}, \dots, v_{s-q-1}, \underbrace{1, \dots, 1}_{q+1}) \end{aligned} \quad (6)$$

where $r = n + p + 1$ and $s = m + q + 1$.

By introducing the piecewise rational basis functions

$$R_{i,j}(u, v) = \frac{N_{i,p}(u) N_{j,q}(v) w_{i,j}}{\sum_{k=0}^n \sum_{l=0}^m N_{k,p}(u) N_{l,q}(v) w_{k,l}} \quad (7)$$

the surface equation (5) can be written as

$$\mathbf{S}(u, v) = \sum_{i=0}^n \sum_{j=0}^m R_{i,j}(u, v) \mathbf{P}_{i,j} \quad (8)$$

Equations (5) to (8) define the evaluation of a point on a NURBS surface, the basic implementation of which is outlined in reference [9].

4.2 NURBS surface tangents and normals

In order to find the normal direction at an arbitrary point on a NURBS surface, the tangential direction in u and v must first be computed using the following equations:

$$\mathbf{T}_u(u, v) = \frac{\partial}{\partial u} \mathbf{S}(u, v) \quad \text{and} \quad \mathbf{T}_v(u, v) = \frac{\partial}{\partial v} \mathbf{S}(u, v) \quad (9)$$

The surface normal is then calculated as the cross-product of the two tangent vectors:

$$\mathbf{N}(u, v) = \mathbf{T}_u(u, v) \times \mathbf{T}_v(u, v) \quad (10)$$

Both equations (9) and (10) were implemented according to Peterson [11]. However, additional modifications were made in collaboration with Peterson, in order to improve the calculation of the magnitude of the partial derivatives.

4.3 Offset NURBS surface

Much of the work that follows makes use of offset NURBS surfaces. An offset surface $\mathbf{O}(u, v)$ is specified by

$$\mathbf{O}(u, v) = \mathbf{S}(u, v) + d\mathbf{N}(u, v)$$

where d is the offset distance. It has been proved [12] that, given a NURBS surface $\mathbf{S}(u, v)$, its offset $\mathbf{O}(u, v)$ is generally not a NURBS. Therefore evaluation of an offset NURBS surface implies a degree of approximation.

In our implementation, the offset surface is constructed using linear least-squares fitting [9]. The method first samples the original surface in the u and v directions, producing a regular grid. The minimum number of samples that has to be taken in order to construct the offset surface is one point per knot span, but it was found that using three points per knot span gave a good balance between speed and accuracy. Each sample point is then projected by a distance d in the direction normal to the surface. Once all of the offset points have been generated the offset surface can then be fitted in least-squares fashion. The parametrization for the new surface is taken directly from the original one. However, in some situations it is necessary to perform knot insertion in order to increase the flexibility of the surface in areas of increased curvature. Regions where knot insertion is required may be identified on the basis of a user-specified tolerance.

5 REGISTRATION OF NURBS MODELS

Registration is the process which establishes point correspondences between the measured data and the entities

of the nominal CAD model. With the data being defined relative to the coordinate frame of the CMM, while the CAD model is defined relative to some other coordinate frame, registration is in the context of this work also taken to signify alignment between the model and the data. Improving the alignment accuracy will reduce the systematic component of the overall measurement error.

Three-dimensional alignment is a non-trivial problem, particularly when dealing with NURBS geometry and large data sets. The adopted solution is based on the modified iterative closest point (ICP) algorithm, which is a realization of least-squares fitting. As the name suggests, ICP is an iterative process to minimize the collective model-part distance, this being the sum of the square distances between the measured points and their corresponding points on the model. At each iteration, it is the point on a model that is closest to the measured one that is taken as corresponding. Thus the algorithm minimizes the following cost function:

$$F = \sum_{i=1}^N |\mathbf{q}_i - \mathbf{R}\mathbf{p}_i - \mathbf{t}|^2 \quad (11)$$

where \mathbf{t} is the translation matrix, \mathbf{R} is the rotation matrix, \mathbf{p}_i is the i th measurement point, \mathbf{q}_i is the closest point on the nominal model and N is the number of measured points. Function minimization is performed using singular value decomposition, to obtain the appropriate geometric transformation that aligns the two objects.

The original ICP algorithm presented in reference [13] was substantially modified by the present authors as reported in reference [14] and its performance was verified against a number of criteria as reported in reference [15]. The resulting implementation was shown to achieve robustness in the presence of measurement noise and high computational efficiency, predominantly through efficient calculation of the closest point on NURBS entity as the time-critical step.

5.1 Validation of the registration method

In the proposed method, the ICP algorithm is applied to align the raw measured data with the offset entities of the CAD model, as an alternative to the conventional approach of having to carry out measurement compensation before performing registration [16]. It is therefore important to compare the registration performance provided by these two approaches. This was performed using the Monte Carlo simulation approach, as described below.

Three orthogonal 20 mm square planes were used to validate registration, being effectively a vertex of a cube. This shape was chosen because it most closely resembles a typical reference feature, comprising three mutually orthogonal flat faces, as required by the

Table 1 Registration accuracy

| | Rotations | | | Translations | | |
|--|-----------|---------|---------|--------------|---------|---------|
| | X (deg) | Y (deg) | Z (deg) | X (mm) | Y (mm) | Z (mm) |
| Standard deviation of the registration error | | | | | | |
| Proposed method | 0.0014 | 0.0004 | 0.0020 | 0.0084 | 0.0095 | 0.0121 |
| Conventional method | 0.1783 | 0.0820 | 0.0676 | 0.0167 | 0.0239 | 0.0166 |
| The mean value of the registration error | | | | | | |
| Proposed method | -0.0001 | 0.0001 | -0.0006 | 0.0037 | -0.0006 | 0.0032 |
| Conventional method | 0.0153 | 0.0268 | -0.0152 | -0.0100 | -0.0220 | -0.0193 |
| The 95% registration accuracy confidence level | | | | | | |
| Proposed method | 0.0009 | 0.0003 | 0.0012 | 0.0052 | 0.0059 | 0.0075 |
| Conventional method | 0.1105 | 0.0508 | 0.0419 | 0.0103 | 0.0148 | 0.0103 |

conventional registration method. Measurements were simulated by sampling a set of 900 evenly distributed points and introducing an offset of 1 mm in the direction of the surface normal to represent the probe offset. No measurement noise was simulated. The model was then transformed randomly 30 times. The transformation was composed of translation and rotation, both values of which were generated as uniformly distributed random numbers within the ranges ± 1 mm and $\pm 1^\circ$ respectively. Misalignment of this magnitude was considered to be representative of practical situations, when an approximate object position can be established relatively easily.

For each misalignment, registration was applied using the proposed offset surface method and the method which uses compensated data. In the latter case the compensation was calculated using the surface normal vectors of the unperturbed model. The registration errors were computed as the differences between the initial perturbation and the results of the registration procedures.

Table 1 presents statistical analysis of the registration errors for the two methods, comparing the standard deviation and mean values of registration error. The results show that the offset surface method produces a consistently higher accuracy of alignment owing to the absence of compensation errors. The same table also presents the 95 per cent confidence intervals for these experiments, further confirming the superior performance of the proposed registration method

6 NURBS SURFACE FITTING

As stated previously, surface fitting is performed for two reasons, namely (a) to produce the offset surfaces of the nominal CAD model, used for registration of the raw measurements, and (b) to construct a surface through raw measured data, used for calculation of the actual surface normals for probe compensation.

In order to fit an approximating surface to the data, a non-linear optimization problem can be set up, with

control points, parameters (u, v) , knots and the weights as unknowns. The objective function to be minimized could be the least-squares error or the maximum error. However, the non-linear nature of the problem can be avoided and the optimization can be greatly simplified if the weights and the knot vector are set *a priori*. Since the nominal CAD model can be regarded as a good approximation of the actual object shape, it is proposed using the control points, weights and knot vectors obtained from the nominal model and then optimizing only the positions of control points. This approach was later shown to achieve both accuracy and computational speed. Following this, the adopted surface approximation method was an extension of that presented by Piegl and Tiller [9] for use with NURBS curves.

By describing the measured points as $\mathbf{Q}_1, \dots, \mathbf{Q}_M$, it is possible to set up and solve the linear least-squares problem for the unknown control points. The cost function to be minimized is

$$f = \sum_{k=1}^M |\mathbf{Q}_k - \mathbf{S}(u_k, v_k)|^2 \quad (12)$$

where u_k and v_k are the parametric coordinates corresponding to each of the measured points. The assignment of these coordinates is crucial because parametrization has a strong effect on the shape of the fitted surface. A number of methods to parametrize measured points have been published [17], but the majority of this work makes the assumption that the data are ordered. Since the present work aims to deal with both ordered and random data, an alternative method was found following the suggestion by Ma and Kruth [17], where the parametrization can be achieved by projecting the points onto a base surface, from which the u_k and v_k values are obtained. The most critical aspect is that each of the points must have a unique projection onto the surface. In this work, the required base surface is readily provided by the entities of the nominal CAD model and the required parametrization is obtained as a result of the ICP registration process.

Substituting equation (8) into equation (12) gives

$$\begin{aligned}
 f &= \sum_{k=1}^M |\mathbf{Q}_k - \mathbf{S}(u_k, v_k)|^2 \\
 &= \sum_{k=1}^M \left| \mathbf{Q}_k - \sum_{i=0}^n \sum_{j=0}^m R_{i,j}(u_k, v_k) \mathbf{P}_{i,j} \right|^2 \\
 &= \sum_{k=1}^M \left[\mathbf{Q}_k \times \mathbf{Q}_k - 2\mathbf{Q}_k \times \sum_{i=0}^n \sum_{j=0}^m R_{i,j}(u_k, v_k) \mathbf{P}_{i,j} \right. \\
 &\quad \left. + \sum_{i=0}^n \sum_{j=0}^m R_{i,j}(u_k, v_k) \mathbf{P}_{i,j} \times \sum_{i=0}^n \sum_{j=0}^m R_{i,j}(u_k, v_k) \mathbf{P}_{i,j} \right]
 \end{aligned} \tag{13}$$

where f is a scalar-valued function of $N = (m+1) \times (n+1)$ variables $\mathbf{P}_{i,j}$. The standard technique of linear least-squares fitting is now applied, while f is minimized by setting the derivatives of f with respect to $\mathbf{P}_{i,j}$ equal to zero:

$$\begin{aligned}
 \frac{\partial f}{\partial \mathbf{P}_{r,s}} &= \sum_{k=1}^M \left[-2\mathbf{Q}_k R_{r,s}(u_k, v_k) \right. \\
 &\quad \left. + 2R_{r,s}(u_k, v_k) \sum_{i=0}^n \sum_{j=0}^m R_{i,j}(u_k, v_k) \mathbf{P}_{i,j} \right]
 \end{aligned}$$

which implies that

$$\begin{aligned}
 &\sum_{k=1}^M \left[R_{r,s}(u_k, v_k) \sum_{i=0}^n \sum_{j=0}^m R_{i,j}(u_k, v_k) \mathbf{P}_{i,j} \right] \\
 &= \sum_{k=1}^M [\mathbf{Q}_k R_{r,s}(u_k, v_k)]
 \end{aligned}$$

Interchanging the order of summation gives

$$\begin{aligned}
 &\sum_{i=1}^n \sum_{j=1}^m \mathbf{P}_{i,j} \sum_{k=1}^M R_{r,s}(u_k, v_k) R_{i,j}(u_k, v_k) \\
 &= \sum_{k=1}^M \mathbf{Q}_k R_{r,s}(u_k, v_k)
 \end{aligned} \tag{14}$$

for $r = 0, \dots, n$ and $s = 0, \dots, m$.

Equation (14) represents one linear equation in the unknowns $\mathbf{P}_{0,0}, \dots, \mathbf{P}_{n,m}$. Letting $r = 0, \dots, n$ and $s = 0, \dots, m$ yields a system of N equations in N unknowns, which can be presented in matrix notation as

$$\mathbf{A}^T \mathbf{A} \mathbf{a} = \mathbf{A}^T \mathbf{b} \tag{15}$$

where \mathbf{A} is the $M \times N$ matrix

$$\mathbf{A} = \begin{bmatrix} R_{0,0}(u_0, v_0) & \cdots & R_{n,m}(u_0, v_0) \\ R_{0,0}(u_1, v_1) & & R_{n,m}(u_1, v_1) \\ \vdots & & \vdots \\ R_{0,0}(u_M, v_M) & \cdots & R_{n,m}(u_M, v_M) \end{bmatrix}$$

and

$$\mathbf{a} = [\mathbf{P}_{0,0} \quad \cdots \quad \mathbf{P}_{n,m}]^T$$

$$\mathbf{b} = [\mathbf{Q}_1 \quad \cdots \quad \mathbf{Q}_M]^T$$

The system of equations (15) has to be solved a total of three times in order to calculate $x_{i,j}$, $y_{i,j}$ and $z_{i,j}$ for all $\mathbf{P}_{i,j}$. If every knot span contains at least one closest point, De Boor [18] shows that $\mathbf{A}^T \mathbf{A}$ is positive definite and well conditioned. Of the many algorithms suggested as a solution to equation (15), an iterative one was chosen, which was implemented using the Gauss–Seidel method. The reasons for this were (a) to take advantage of the initial estimate for the position of the control points provided by the nominal model and (b) to minimize computational error within the solution of such large matrices [19].

Fitting complex surfaces through large measurement data sets can be expensive in terms of both computation time and memory, a significant proportion of which can be attributed to the matrix multiplication $\mathbf{A}^T \mathbf{A}$. The time and memory requirements can be drastically reduced by exploiting the sparse and banded nature of \mathbf{A} . This means that only non-zero elements of \mathbf{A} are stored and directly multiplied. As a result it is possible to reduce both the number of computations and the memory requirements.

7 SIMULATION STUDIES

Following implementation of the functionality described above, the objective was to evaluate the performance of the proposed compensation method in relation to the conventional one. In particular, the aim was to investigate the accuracy of the two methods in the presence of:

- shape deformation and
- positional misalignment.

These two effects were investigated separately. In both cases the nominal object shape was a part of a cylinder (Fig. 7), which was chosen because it can be modelled precisely using NURBS with unequal weights, it can be readily manufactured with high precision and it allows full investigation of the effects of interest.

In each case simulation involved probe tip radius of 1 mm. The measurement points were evenly distributed over a grid of 100×100 points. The noise characteristic was Gaussian, with a standard deviation between 0 and $40 \mu\text{m}$.

In terms of the computing time, the dominant step in the proposed procedure was found to be the fitting of the NURBS surface. The simulation experiments involved 10 000 measured points and NURBS with approximately 150 control points. The corresponding

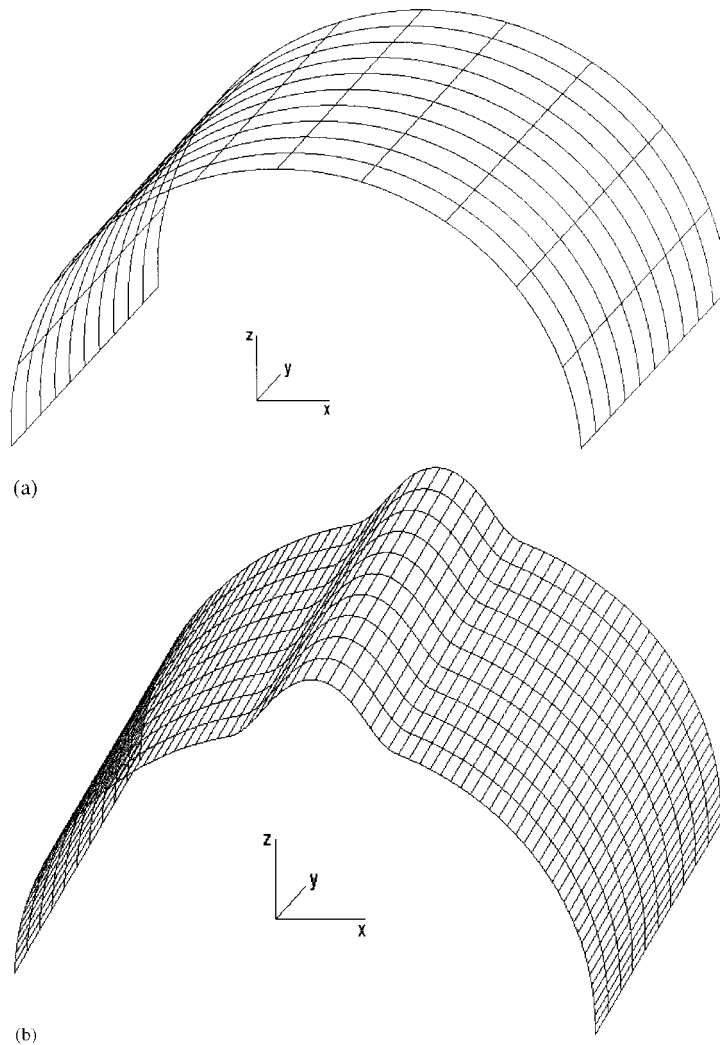


Fig. 7 Models used in simulation studies: (a) nominal shape and (b) deformed shape, magnitude = 1 mm

computing time on a 200 MHz Pentium machine was under 1 min.

7.1 Effect of misalignment

This analysis required two surfaces to be used, namely (a) the surface representing the nominal CAD model of the part and (b) the offset nominal surface, where offset equals probe radius. Only one gross misalignment value of -2 mm translation in the z direction was simulated, because registration accuracy had already been assessed as presented in Section 4 and here it was only necessary to investigate the combined effects of misalignment and measurement noise. The simulation procedure can therefore be summarized as follows:

1. Import the nominal model of the component into the simulation software.
2. Import the offset nominal model and apply the simulated misalignment.
3. On the basis of the required measurement point density, calculate the measurement point locations on the nominal model and their normal direction from this model.
4. Using the measurement points and normals calculated in the previous step, project lines away from the nominal model toward the offset.
5. Calculating the intersection between these projection lines and the offset surface will yield the actual raw (uncompensated) measurement that would be taken by the CMM under such misalignment conditions.
6. Apply compensation.
7. Apply the simulated misalignment to the nominal model.
8. The compensation error is obtained by calculating the distance between each compensated point and the nominal model.

Simulation results are presented in Fig. 8, showing the average and the standard deviation of the compensation

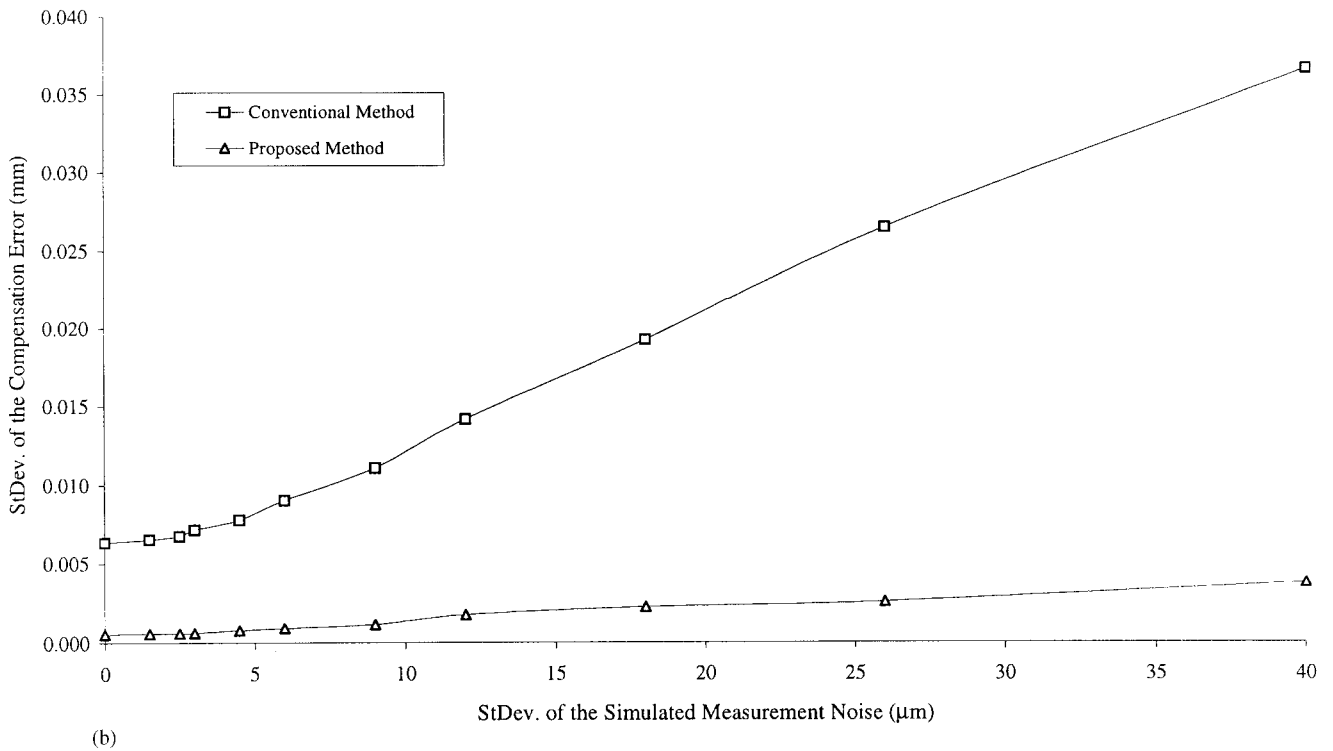
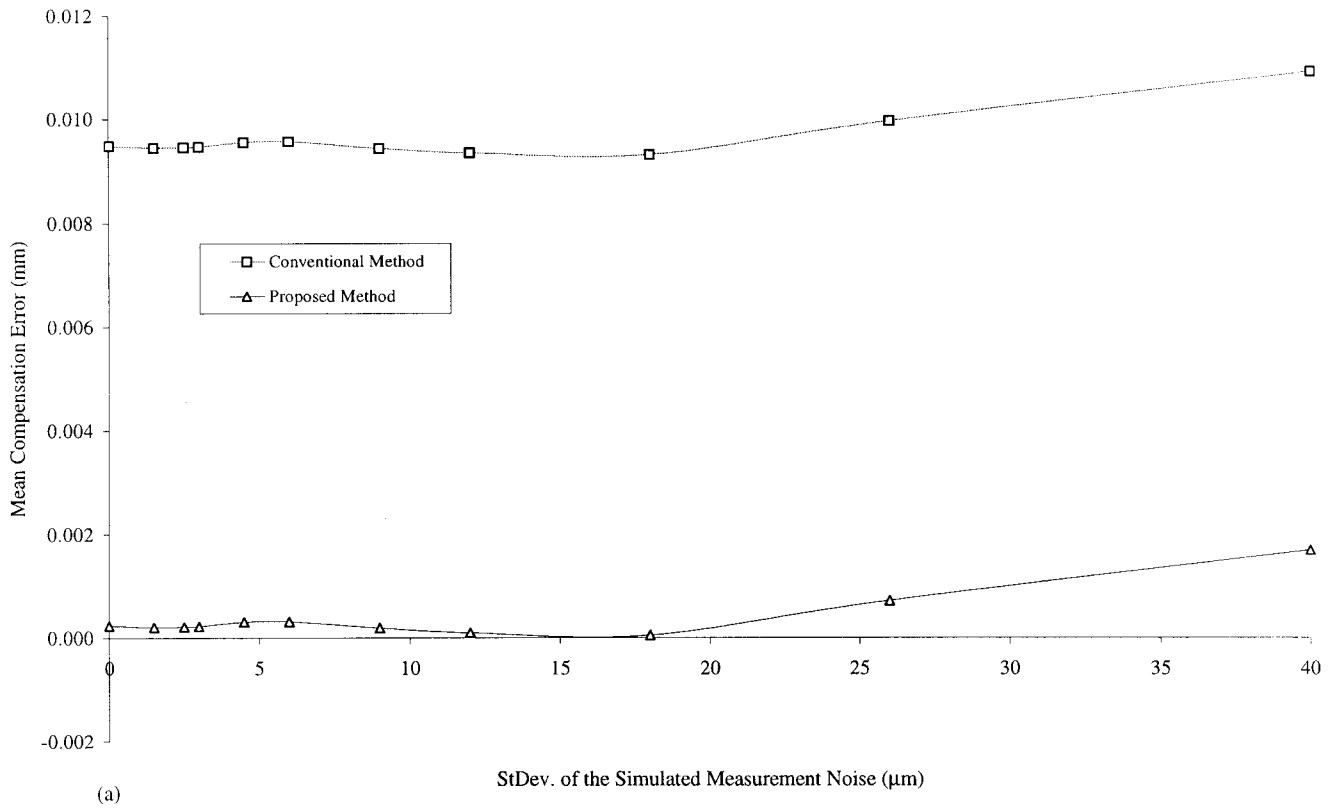


Fig. 8 Effects of object misalignment and measurement noise: (a) mean and (b) standard deviation

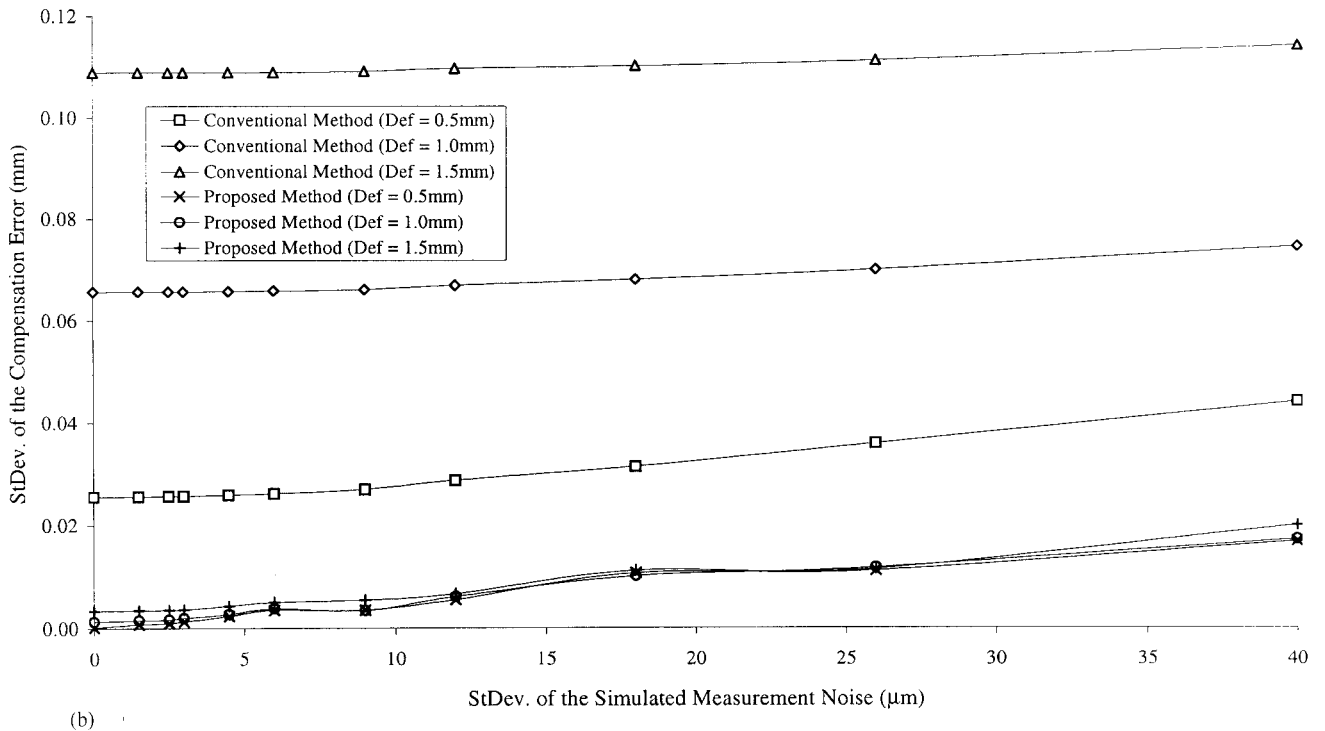
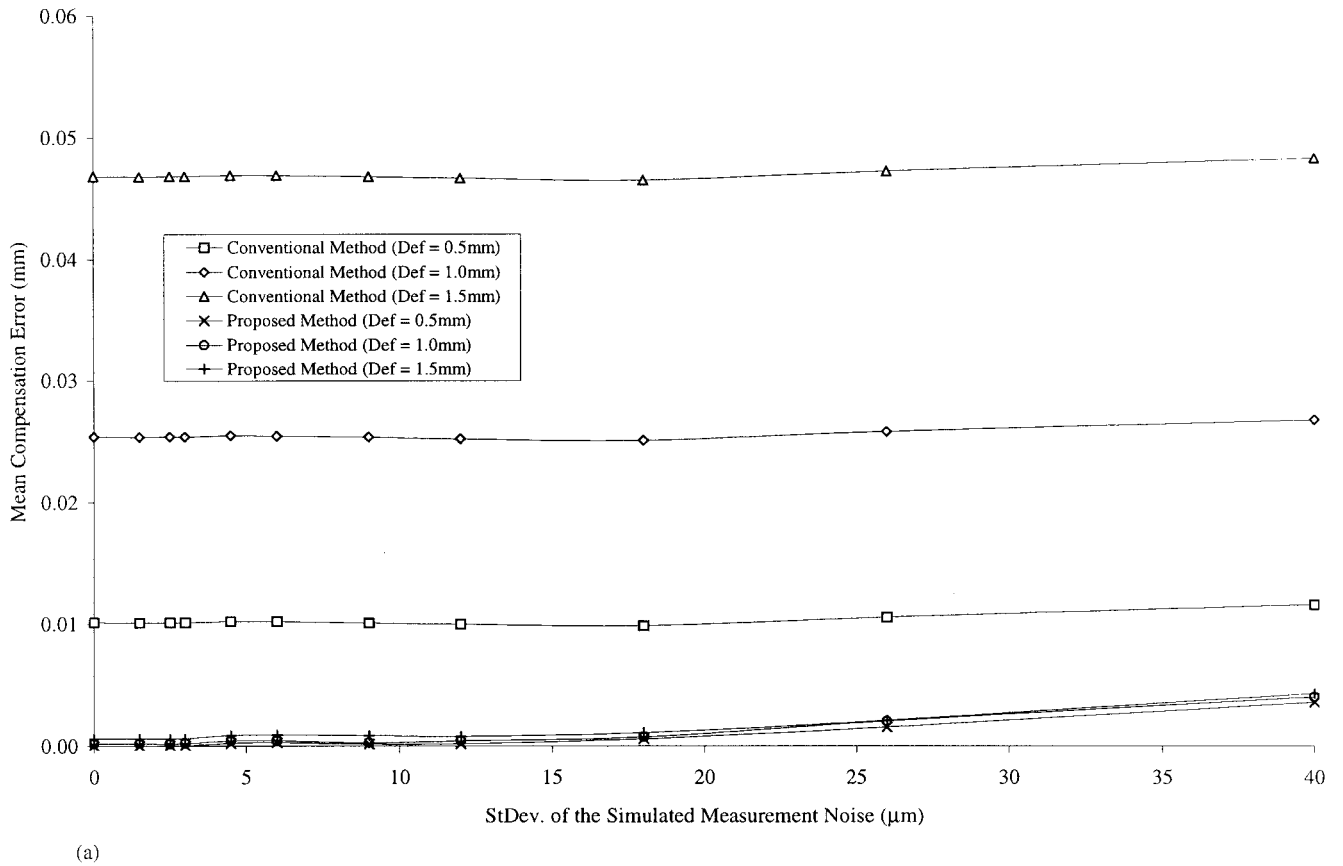


Fig. 9 Effects of object deformation and measurement noise: (a) mean and (b) standard deviation

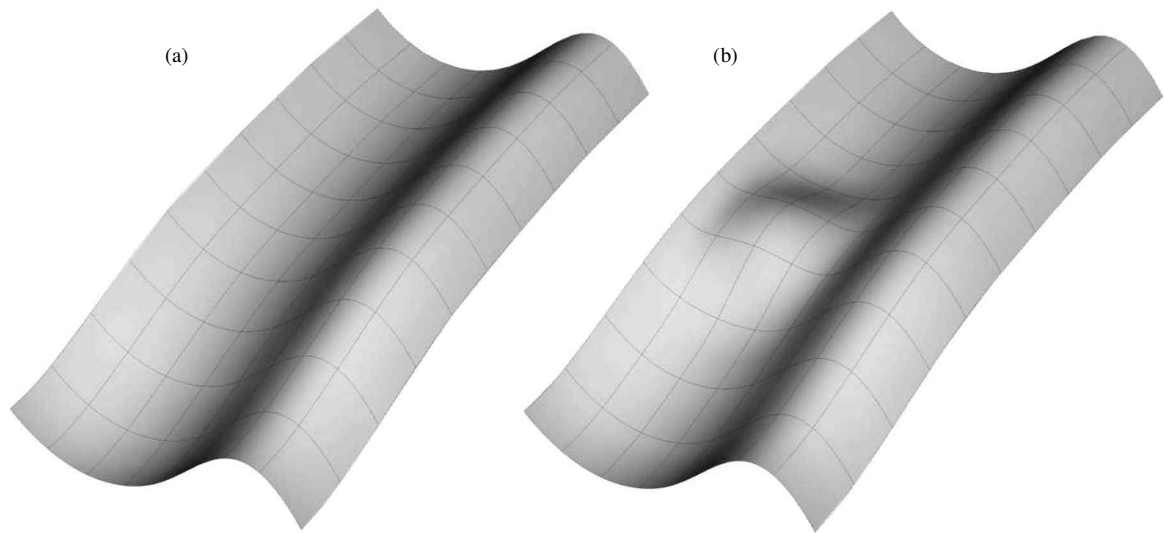


Fig. 10 Model surfaces used for free-form compensation: (a) nominal surface and (b) deformed surface

error. Figure 8a shows that the proposed method achieves consistently better average errors and this is expected on the basis of the improved registration. Figure 8b shows that standard deviation is also significantly better and this may be expected as a result of the data smoothing.

7.2 Effect of deformation

This analysis required three surfaces to be used, namely (a) the nominal CAD model surface, (b) the deformed surface representing the actual part and (c) the deformed surface offset by the probe radius. The shape of the deformed surface is shown in Fig. 7b, indicating local deformation of a sinusoid profile. Three deformation magnitudes were applied, with the sinusoid profile peak values 0.5, 1.0 and 1.5 mm. The overall simulation procedure can be summarized as follows:

1. Import the nominal model of the component.
2. Import the offset deformed model.

3. On the basis of the required measurement point density, calculate the measurement point locations on the nominal model and their normal direction from this model.
4. Using the measurement points and normals calculated in the previous step, project lines away from the nominal model toward the offset deformed model.
5. Calculating the intersection between these projection lines and the offset deformed surface will yield the actual raw (uncompensated) measurement that would be taken by the CMM under such deformation conditions.
6. Perform compensation.
7. Import the deformed model.
8. The compensation error is obtained by calculating the distance between each compensated point and the deformed model.

Simulation results are presented in Fig. 9 showing the average and the standard deviation of the compensation error for different deformations and different

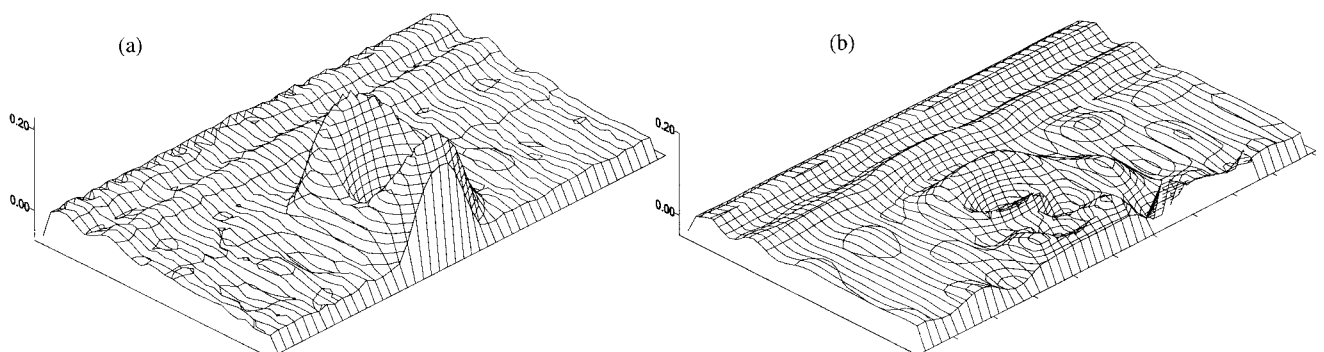


Fig. 11 Error analysis for free-form surface compensation: (a) conventional compensation and (b) the proposed method of compensation

Table 2 Comparison of compensation errors using the conventional and the proposed method

| | Conventional compensation error (mm) | Proposed compensation error (mm) |
|--------------------|--------------------------------------|----------------------------------|
| Standard deviation | 0.045 965 | 0.012 947 |
| Mean | -0.018 314 | -0.003 014 |
| Minimum | -0.049 | -0.055 |
| Maximum | 0.279 | 0.094 |

measurement noise values. These figures clearly demonstrate the superior compensation accuracy achieved by the proposed method in all cases.

7.3 A free-form surface example

Finally, a case study is presented involving a true free-form shape. The compensation was performed in the presence of both misalignment and surface deformation. The surfaces used can be seen in Figs 10a, representing the nominal surface, and 10b, representing the actual, deformed surface. A misalignment transformation consisting of -0.2 mm translation (dz) and a 1.5° rotation about the y axis was applied. A measurement point mesh consisting of 120×60 points evenly distributed across the surface was used. The probe tip radius was 1 mm, and measurement noise was introduced with a standard deviation of $4.5 \mu\text{m}$. Figure 11 shows the error analysis of the compensated data points, comparing the conventional and the proposed methods. It can be seen that the proposed method achieves a significant improvement in accuracy. Table 2 presents the statistical data for the compensation error in this example.

8 CONCLUSION

The paper has presented implementation and performance analysis of a CAD-based method for probe radius compensation. The method was designed to deal with difficult situations which arise when performing dimensional measurement on free-form geometry, particularly in cases when the part in question possesses no clear reference features and when it is appreciably deformed in relation to its nominal shape. This is characteristic of numerous applications in engineering manufacture. Importantly, the method makes no assumptions regarding distribution of the measured points, other than that the data sufficiently well represent the underlying object shape. Furthermore, the method is capable of producing accurate results in the presence of appreciable measurement noise. Experimentation using an available CMM system was used to obtain typical measurement error characteristics for an instrument of that type and these results helped in defining the

parameters for a simulation study. The performance of the proposed method was analysed on the basis of detailed simulation studies and compared with the conventional method, clearly demonstrating superior results. The proposed method is considered to be also applicable to other types of contact measuring systems in addition to the CMM.

REFERENCES

- 1 Menq, C. H., Yau, H. T. and Wong, C. L. An intelligent planning environment for automated dimensional inspection using coordinate measuring machines. *Trans. ASME, J. Engng for Industry*, May 1992, **114**(2), 222–230.
- 2 Pahk, H. J., Jung, M. Y., Hwang, S. W., Kim, Y. H., Hong, Y. S. and Kim, S. G. Integrated precision inspection system for manufacturing of moulds having CAD defined features. *Int. J. Adv. Mfg Technol.*, 1995, **10**(3), 98–207.
- 3 Faux, I. D. and Pratt, M. J. *Computational Geometry for Design and Manufacture*, 1979, p. 268 (Ellis Horwood, Chichester).
- 4 Song, C. K. and Kim, S. W. Reverse engineering: autonomous digitization of free-formed surfaces on a CNC coordinate measuring machine. *Int. J. Mach. Tools Mf.*, 1997, **37**(7), 1041–1051.
- 5 Ainsworth, I., Ristic, M. and Brujic, D. Visual CAD-based measurement and path planning for free-form shapes. In 7th International Conference in Central Europe on *Computer Graphics, Visualisation and Interactive Digital Media*, WSCG '99, Prague, Czech Republic, 8–12 February 1999.
- 6 Anoyama, H. and Kawa, M. A new method for detecting the contact point between a touch probe and a surface. *Ann. CIRP*, 1989, **38**(1), 517–520.
- 7 Mayer, J. R., Mir, Y. A., Trochu, F., Vafaeesefat, A. and Balazinski, M. Touch probe radius compensation for coordinate measurement using Kriging interpolation. *Proc. Instn Mech. Engrs, Part B, Journal of Engineering Manufacture*, 1997, **211**(B1), 11–18.
- 8 ANSI/CAM-I 101-1995 *Dimensional Measuring Interface Standard*, revision 3.0, 1995 (Consortium for Advanced Manufacturing).
- 9 Piegl, L. A. and Tiller, W. *The NURBS Book*, 2nd edition, 1997 (Springer, Berlin).
- 10 ANSI Y14.26M *The Initial Graphics Exchange Specification (IGES)*, Version 5.2, 1993 (U.S. Product Data Association, Fairfax, Virginia).
- 11 Peterson, J. W. Tessellation of NURBS surfaces. In *Graphic Gems IV* (Ed. P. S. Heckbert), 1994, pp. 287–319 (Academic Press, New York).
- 12 Piegl, L. A. and Tiller, W. Computing offsets of NURBS curves and surfaces. *Computer-Aided Des.*, 1999, **31**, 147–156.
- 13 Besl, P. J. and McKay, N. D. A method for registration of 3-D shapes. *IEEE Trans. Pattern Analysis Mach. Intell.*, February 1992, **14**(2), 239–256.
- 14 Ristic, M. and Brujic, D. Efficient registration of NURBS geometry. *Int. J. Image Vision Comput.*, 1997, **15**, 925–935.
- 15 Ristic, M. and Brujic, D. Analysis of free form surface registration. *Proc. Instn Mech. Engrs, Part B, Journal of Engineering Manufacture*, 1997, **211**(B8), 605–617.

- 16 **Sahoo, K. C.** and **Menq, C. H.** Localization of 3-D objects having complex sculptured surfaces using tactile sensing and surface description. *J. Engng for Industry*, February 1991, **113**, 85–92.
- 17 **Ma, W.** and **Kruth, J. P.** Parameterization of randomly measured points for least squares fitting of *B*-spline curves and surfaces. *Computer-Aided Des.*, 1995, **27**(9), 663–675.
- 18 **De Boor, C.** Gauss elimination by segments and multivariate polynomial interpolation. In Purdue Conference on *Approximation and Computation*, 2–5 December 1993.
- 19 **Press, W. H., Teukolsky, S. A., Vetterling, W. T.** and **Flannery, B. P.** *Numerical Recipes in C: The Art of Scientific Computing*, 2nd edition, 1993 (Cambridge University Press, Cambridge).